

From Pixels to Tokens: Revisiting Object Hallucinations in Large Vision-Language Models

Yuying Shang*
shangyuying21@mails.ucas.ac.cn
University of Chinese Academy of
Sciences
Beijing, China

Xinyi Zeng*
Dept. of Comp. Sci. and Tech.,
Institute for AI, Tsinghua University
Beijing, China

Yutao Zhu*
Gaoling School of Artificial
Intelligence, Renmin University of
China
Beijing, China

Xiao Yang
Dept. of Comp. Sci. and Tech.,
Institute for AI, Tsinghua University
Beijing, China

Zhengwei Fang
Dept. of Comp. Sci. and Tech.,
Institute for AI, Tsinghua University
Beijing, China

Jingyuan Zhang
Kuaishou Technology Inc.
Beijing, China

Jiawei Chen
Shanghai Key Laboratory of Multi.
Info. Processing, East China Normal
University
Shanghai, China

Zinan Liu
University of Chinese Academy of
Sciences
Beijing, China

Yu Tian[†]
tianyuan1810613@gmail.com
Dept. of Comp. Sci. and Tech.,
Institute for AI, Tsinghua University
Beijing, China

Abstract

Hallucination in large vision-language models (LVLMs) is a significant challenge, *i.e.*, generating objects that are not present in the visual input, which significantly compromises the reliability of models. Recent studies often attribute hallucinations to a lack of visual understanding, yet ignore a more fundamental issue: the model's inability to effectively extract or decouple visual features. In this paper, we revisit the hallucinations in LVLMs from an architectural perspective, investigating whether the primary cause lies in the visual encoder (feature extraction) or the modal alignment module (feature decoupling). Motivated by our preliminary findings, we propose a parameter-efficient fine-tuning strategy, PATCH, to mitigate hallucinations in LVLMs. This plug-and-play method can be integrated into various LVLMs, leveraging adaptive virtual tokens to extract object features from bounding boxes, thereby addressing hallucinations stemming from inadequate feature decoupling. PATCH achieves state-of-the-art performance across multiple multi-modal hallucination datasets and demonstrates significant improvements in general capabilities. We hope this work provides deeper insights into the underlying causes of hallucinations in LVLMs, fostering further advancements and innovation in this field. The code will be available at <https://github.com/YuyingShang/PATCH>.

CCS Concepts

• **Computing methodologies** → Reasoning about belief and knowledge; *Natural language generation*.

*Both authors contributed equally to this research.

[†] Corresponding author.



This work is licensed under a Creative Commons Attribution 4.0 International License.
MM '25, Dublin, Ireland

© 2025 Copyright held by the owner/author(s).
ACM ISBN 979-8-4007-2035-2/2025/10
<https://doi.org/10.1145/3746027.3755728>

Keywords

large vision language model; hallucination; virtual token

ACM Reference Format:

Yuying Shang, Xinyi Zeng, Yutao Zhu, Xiao Yang, Zhengwei Fang, Jingyuan Zhang, Jiawei Chen, Zinan Liu, and Yu Tian. 2025. From Pixels to Tokens: Revisiting Object Hallucinations in Large Vision-Language Models. In *Proceedings of the 33rd ACM International Conference on Multimedia (MM '25)*, October 27–31, 2025, Dublin, Ireland. ACM, New York, NY, USA, 11 pages. <https://doi.org/10.1145/3746027.3755728>

1 Introduction

Large vision-language models (LVLMs) have achieved remarkable performance across a broad range of tasks, even surpassing human capabilities in certain scenarios [19, 37, 44]. However, their practical applications are often hindered by multi-modal hallucinations, where models generate factually incorrect or entirely fictitious outputs when interpreting visual features. Recently, various methods have been proposed to address hallucinations in LVLMs, focusing on aspects such as data distribution [17, 42], training scheme [34, 46], and decoding strategy [39, 45]. Despite these advancements, a fundamental question remains unexplored: **What is the primary cause of multi-modal hallucinations?**

To better address the problem, we start by exploring the intrinsic sources of hallucinations in LVLMs. We hypothesize two potential factors: (1) insufficient extraction of visual features and (2) inadequate decoupling of these features during multi-modal integration. To validate this, we revisit hallucinations in LVLMs from an architectural perspective, focusing on two key components: the visual encoder (responsible for feature extraction) and the modal alignment module (responsible for feature decoupling). First, we assess the role of the visual encoder by combining it with a pre-trained object detection head to perform object recognition on a hallucination dataset. The detected results are then compared with the

Table 1: Comparison between the number of samples in detection and inference results, where “Det.” denotes Detection and “Inf.” denotes Inference.

	Correct Inf.	Wrong Inf.
Correct Det.	2,396	308
Wrong Det.	105	191

direct inference outputs of the LVLM on the same dataset. Our analysis reveals that the primary source of object hallucinations lies in insufficient cross-modal alignment at the modal alignment module, rather than limitations in the encoding capacity of the visual encoder. Subsequently, we augment the LVLM’s input sequence with object-related information, demonstrating that the model’s resistance to hallucinations is effectively improved.

Motivated by the preliminary findings, we propose a novel fine-tuning strategy to mitigate hallucinations in LVLMs named **PATCH** (Pluggable virtuAl Tokens for objeCt Hallucinations). PATCH is designed to enable LVLMs to better leverage object-related information, aligning visual and textual features in the semantic space to mitigate object hallucinations. Concretely, PATCH introduces trainable and pluggable virtual tokens between image features and enhanced prompt texts, bridging the gap between the encoded image features and input-augmented texts with minimal parameter tuning. During inference, the fine-tuned virtual token embeddings are added to the original vocabulary, making PATCH a plug-and-play method that is adaptable to various application scenarios.

To validate the effectiveness and generalization of our method, we conduct experiments on three publicly available multi-modal hallucination evaluation datasets across three LVLMs. Notably, when enhancing the LLaVA-v1.5 [22], MiniGPT-4 [48], and MiniGPT-v2 [7] with PATCH, the accuracy scores on the POPE [21] dataset have surged from 85.17% to 90.20% (an absolute improvement of 5.03%), 57.67% to 88.13% (an absolute improvement of 30.46%), and 83.33% to 90.03% (an absolute improvement of 6.70%).

Our experiments and methodology have provided an insightful exploration of the fundamental causes of multi-modal hallucinations from a new perspective, offering new ideas for solving multi-modal hallucinations in LVLMs. In summary, our contributions are summarized as follows: (1) We explore the intrinsic sources of hallucinations in LVLMs, revealing that the inadequate decoupling of textual and visual features during multi-modal integration is the primary factor behind hallucinations in LVLMs. (2) We propose PATCH, a parameter-efficient fine-tuning strategy, which enables LVLMs to more effectively leverage visual detection information to address hallucination issues. (3) The effectiveness of PATCH has been validated on three multi-modal hallucination evaluation datasets across three LVLMs, and further exploration of various hallucination types has demonstrated its great potential, especially in handling strong misleading difficulty in questions.

2 Related Work

2.1 Large Vision-Language Models

Large Vision-Language Models (LVLMs) represent a significant advancement in multi-modal artificial intelligence, combining visual perception and natural language understanding to process

Table 2: Inference results of MiniGPT-v2 using Prompt₁ and Prompt₂ on the POPE dataset.

	Accuracy	F1
Prompt ₁	0.833	0.822
Prompt ₂	0.888	0.888

and generate contextual information. The typical LVLM architecture primarily consists of a large language model [35, 36] for text processing and a visual encoder [12, 28, 31] for feature extraction. By incorporating various cross-modal alignment mechanisms, such as MLP [33], attention mechanism [1], and Q-Former [9, 19], LVLMs achieve seamless integration between visual and textual embeddings. In recent years, LVLMs have demonstrated remarkable performance across multiple tasks, particularly in image captioning [8, 30], visual question answering [20, 38], and visual reasoning and generation [4]. Models like InstructBLIP [9], MiniGPT [7, 48], and LLaVA [23] leverage pretrained cross-modal feature alignment and the instruction fine-tuning strategy to enhance the vision-language representation synergy, improving the model’s ability in complex instruction comprehension. However, empirical studies reveal that current LVLMs suffer from hallucination issues, frequently generating descriptions containing objects absent from the input visual content [2, 24]. In this paper, we conduct systematic experimental analysis to explore the underlying cause of hallucination in LVLMs, proposing a novel fine-tuning strategy to alleviate the object hallucination issue in LVLMs.

2.2 Object Hallucinations in LVLMs

Hallucination refers to the generation of irrelevant, factually inconsistent, or semantically meaningless content relative to the given context [5, 26]. For LVLMs, this phenomenon primarily manifests as the misalignment between the generated textual descriptions and the corresponding visual input. Recent research has increasingly focused on addressing this critical challenge to improve LVLM reliability. Tong et al. [34] explored the gap between the visual embedding space of CLIP and vision-only self-supervised learning, identifying that the insufficient visual comprehension is the primary factor for multi-modal hallucination. Jiang et al. [17] further analyzed the representation distribution in LVLMs for both text and visual tokens, revealing the significant misalignment in cross-modal representations. Zhou et al. [47] examined the hallucinated textual outputs of LVLMs, finding that the object hallucination issue is closely correlated with the inherent uncertainties during the beam search processes, suggesting that both data distribution and decoding methods contribute to the hallucination issue.

Building upon these findings, current hallucination mitigation approaches primarily focus on optimizing the data distribution [17, 42], improving the training paradigm [6, 16, 46], employing human feedback [18, 32], and designing novel decoding strategies [39, 45]. However, these methods frequently encounter limitations, including excessive computational resources and data requirements, and the reliance on manually engineered fine-tuning prompts. In contrast to existing approaches, we propose PATCH, a novel

parameter-efficient tuning strategy, which revisits LVLm hallucinations through architectural perspective, effectively mitigating multi-modal hallucination across diverse application scenarios.

3 Analysis of Object Hallucinations in LVLms

We first hypothesize two potential sources of multi-modal object hallucinations in LVLms. Then, we design and conduct a series of experiments to quantify the impact of these sources. Finally, we thoroughly discuss and analyze the experimental results, offering a solution to mitigate the hallucination issue.

3.1 Potential Sources of Hallucination

The architecture of LVLms typically consists of three components: a visual encoder, a visual projection layer, and a large language model (LLM). The visual encoder is responsible for extracting image features, while the visual projection layer decouples and aligns these features with the semantic space of the LLM. The LLM is responsible for interpreting both the text and image features to generate appropriate responses. Since both the visual encoder and the visual projection layer process image information, they are inherently prone to introducing object hallucinations. Therefore, we hypothesize that multi-modal object hallucinations in LVLms stem from two main sources: (1) **Insufficient extraction of visual features.** The visual encoder may fail to capture critical details or misinterpret objects within the image, leading to inaccurate or incomplete visual representations. (2) **Inadequate decoupling of visual features.** Even when the visual encoder extracts accurate features, the visual projection layer may struggle to correctly align them with the corresponding textual embeddings in the joint semantic space. This misalignment hinders the LLM’s ability to integrate and interpret visual information, resulting in hallucinatory outputs. To investigate the root source of the hallucinations, we design and conduct the following experiments.

3.2 Empirical Analysis

Object Hallucination Dataset. Our experiments are conducted on the POPE [21] dataset, a dedicated dataset for assessing object hallucination in vision-language models. The dataset consists of 3,000 samples that are highly related to the presence condition of objects within an image. The evaluation is formulated as a binary classification task, where the model is prompted to respond with “yes” or “no” to questions such as, “*Is there a bicycle in the image?*” Given the binary labels, we can directly assess whether the model is hallucinating or not without applying complex parsing rules. A model is considered to be hallucinating if it answers “yes” for an object not present in the image, or “no” for an object that is present.

Experimental Setup. We conduct a preliminary experiment by MiniGPT-v2 [7], which employs a Vision Transformer (ViT) [11] as its visual encoder. To validate the image encoding capability of MiniGPT-v2’s visual module, we combine it with a pre-trained Cascade Mask R-CNN [3] head, which serves as the object recognition model. We design a prompt, denoted as Prompt₁, to evaluate the zero-shot inference performance of MiniGPT-v2, formulated as: `[Image][vqa][Question]`, where [Image] and [Question] are placeholders for the input image and question, while [vqa] serves as MiniGPT-v2’s task identifier. To quantify the

alignment between detection and inference, we count the number of correctly and incorrectly identified samples inferred by the model, as shown in Table 1. Ideally, the correct object detections should correspond to accurate model outcomes, while incorrect detections should result in faulty inferences. Any deviation or inconsistency between the detected objects and the model’s final inference results is regarded as an instance of object hallucination.

Analysis. As shown in Table 1, 413 samples (308 correct detections with incorrect inferences and 105 incorrect detections) exhibit object hallucinations in MiniGPT-v2, accounting for 13.77% of the total dataset. Notably, 74.58% of these cases arise when object detection is accurate while the model’s inference is incorrect, indicating this as the predominant failure mode.

This finding suggests that while MiniGPT-v2’s visual encoder is able to extract accurate image features, its visual projection module struggles to seamlessly bridge the encoded features with the LLM’s semantic space. The fundamental misalignment between visual feature encoding and the LLM’s semantic interpretation constitutes a primary factor contributing to multi-modal object hallucinations.

Potential Solutions. In many computer vision tasks [10, 15], objects are typically characterized by their categories and bounding boxes. We hypothesize that incorporating object-related information directly into the prompt texts can mitigate the misalignment between visual features and the LLM’s semantic space, improving the model’s understanding of objects in images. To test this hypothesis, we conduct an additional experiment using a modified prompt, denoted as Prompt₂: `[Image]Objects: [Object][vqa][Question]`. The object-related information is inserted at the [Object] position, formatted as `category{<x1><x2><x3><x4>}`, where each detected object category is concatenated with its corresponding bounding boxes. This inclusion of object recognition details is intended to enhance the LLM’s ability to comprehend and process the object information within images. Table 2 shows the results of MiniGPT-v2 based on Prompt₁ and Prompt₂. It is evident that incorporating accurate detection information significantly improves the model’s performance on questions related to object existence, thus enhancing its image interpretation capability and effectively reducing object hallucinations.

Motivation. While our preliminary experiments identify the potential causes of object hallucinations and suggest a possible solution, we observe that directly incorporating detection information into the input may introduce unnecessary details, particularly when detected objects are weakly correlated with the given question. This redundancy may interfere with the model’s reasoning process, hindering its ability to effectively utilize relevant information. To address this issue, we propose the PATCH tuning strategy, which employs trainable and pluggable virtual tokens to help the LLM selectively optimize the use of detection information. These virtual tokens serve as a bridge, allowing LVLms to focus on task-relevant image features, improving alignment between visual and textual representations within the semantic space.

4 Methodology

In this section, we first introduce the task formulation and then provide a comprehensive description of our method, including its theoretical foundations and practical implementation.

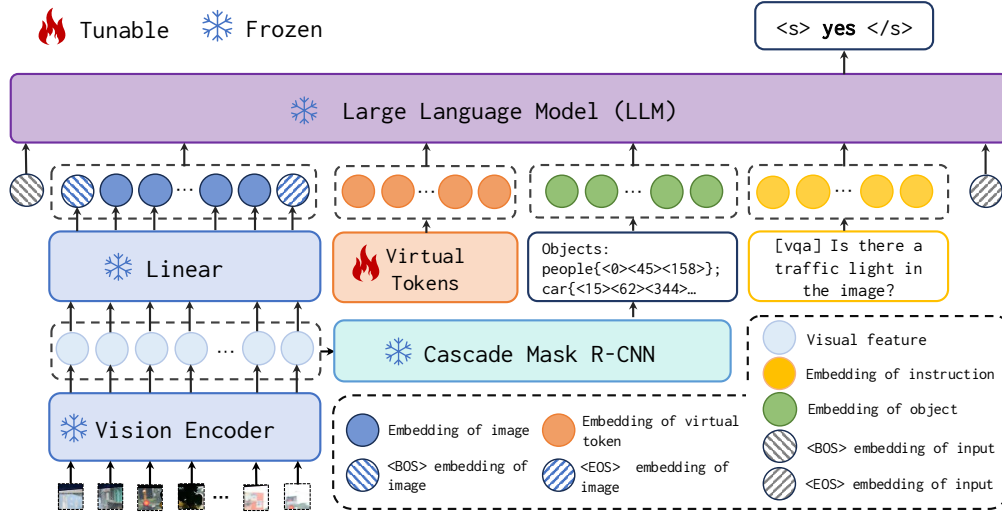


Figure 1: The architecture of LVLMs with PATCH (taking MiniGPT-v2 as an example) where the visual encoder, linear projection layer, and the LLM remain frozen during the fine-tuning phase. The only updated component is the parameters of the virtual tokens. A frozen pre-trained Cascade Mask R-CNN head is adopted to obtain the object-related information in the test images.

4.1 Problem Formulation

The LVLMs aim to generate proper text responses to multi-modal inputs by integrating visual and textual information. The standard approach involves extracting visual features through a visual encoder, mapping these features into the linguistic semantic space via a projection layer for cross-modal fusion and alignment. The fused representations are then decoded by an autoregressive language model to generate the final response. Formally, given an input image I and a corresponding question or text prompt Q , the generated answer sequence Y is calculated as:

$$p(Y) = \prod_{t=1}^T p_{\theta}(y_t | I, Q, y_{<t}), \quad (1)$$

where $y_{<t}$ denotes the sequence of tokens prior to the current token y_t at step t , and θ represents the parameters of the LVM. Based on our preliminary analysis, we observe that incorporating object categories C and their corresponding bounding boxes B can enhance the generation process. Therefore, the generation process can be reformulated as:

$$p(Y) = \prod_{t=1}^T p_{\theta}(y_t | I, D, Q, y_{<t}), \quad (2)$$

where $D = [C(I); B(I)]$. In the object hallucination recognition task, the input question Q is designed to assess the presence of hallucinated objects. The task aims to generate the correct answer Y by evaluating whether a given object appears in the image I .

4.2 PATCH

The proposed fine-tuning strategy aims to mitigate object hallucinations in LVLMs by introducing trainable virtual tokens that leverage additional object-related information. The architecture of our method (taking MiniGPT-v2 as an example) is illustrated in Figure 1. Inspired by [49], we insert a set of n virtual tokens

$T = [t_1, t_2, \dots, t_n]$ between the image features and the detection information D . These token embeddings are optimized during training, with parameters $\delta \in \mathcal{R}^{n \times d}$, where d is the embedding dimension of the LVM. The generation process of LVLMs, augmented by these virtual tokens, is formulated as:

$$p(Y) = \prod_{t=1}^T p_{\delta, \theta}(y_t | I, [t_1, t_2, \dots, t_n], D, Q, y_{<t}). \quad (3)$$

To reduce the computing resources, all LVM parameters θ are frozen during fine-tuning, except for the newly introduced parameters δ of virtual tokens. For instance, with 20 additional virtual tokens, only $20 \times 4,096 = 0.08\text{M}$ parameters are trainable, accounting for merely 0.0012% of the total model parameters. This approach achieves substantial computational efficiency while preserving its optimization capability for object hallucination mitigation. Comprehensive experimental analysis is demonstrated in Section 5.4.

During the inference phase, we extend the model's vocabulary by incorporating several special tokens (e.g., [ref1], [ref2], ..., [refn]) whose embeddings are initialized by the fine-tuned virtual token embeddings. This makes PATCH a plug-and-play method that can be dynamically adjusted based on application requirements. Specifically, when object-related information is included in the users' input, virtual tokens can be added before the detection results, helping to mitigate object hallucinations in LVLMs. Conversely, when no additional detection information is provided, the LVM can revert to processing the input using its standard capabilities without PATCH involvement. PATCH strengthens image comprehension by optimizing the alignment between visual features and textual semantics while preserving the model's inherent capabilities. This adaptability is particularly valuable in practical applications, as LVLMs are commonly deployed across diverse downstream tasks. By narrowing the representational gap between modalities, PATCH improves cross-modal feature fusion, particularly for tasks that

benefit from enriched detection prompts, ultimately reducing object hallucinations and enhancing the overall performance of LVLMs.

5 Experiments

5.1 Datasets

To verify the effectiveness of our method, we conduct experiments on two publicly available multi-modal hallucination evaluation datasets. (1) **POPE** dataset [21] is specifically designed for evaluating object hallucinations in LVLMs, which comprises 3,000 adversarially constructed samples from A-OKVQA and MSCOCO, respectively. The A-OKVQA portion is treated as the training set, while the MSCOCO portion is for testing. (2) **PhD** dataset [25] is a newly introduced benchmark for multi-modal hallucination evaluation. We conduct experiments on its v1 version across five task types that are highly related to objects, including Object Recognition, Attribute Recognition, Counting, Positional Reasoning, and Sentiment Analysis. 80% of the data are randomly selected for training, while the rest is for testing.

5.2 Implementation Details

The LLaVA-v1.5, MiniGPT-4, and MiniGPT-v2 are adopted as the backbone LVLMs, initializing them with their default parameter configurations. Given the advanced capabilities of MiniGPT-v2, most of our experiments are conducted by this model. Accuracy, Precision, Recall, and F1 score are employed as evaluation metrics. The cosine scheduler [27] is utilized to adjust the learning rate and the LLaMA-2-7B-chat [35] is employed as the language model.

All backbone models are fine-tuned over $20 \times d$ trainable parameters by default, where d represents the dimensionality of the hidden layers. As demonstrated in our preliminary experiments (Section 3.2), incorporating object-related information directly into the input prompt (Prompt₂) can also improve performance. We refer to this simple approach as the “**Hard Prompt**” method. All training is performed on a single NVIDIA A100 GPU.

5.3 Baselines

We consider nine mainstream LVLMs: (1) **mPLUG-Owl** [40] is a two-stage training framework that aligns visual and textual modalities by training a visual knowledge module followed by an abstraction module. (2) **Multi-modal-GPT** [14] utilizes a specially designed input sequence and calculates the loss based on the response and the end token to enhance visual-text alignment. (3) **InstructBLIP** [9] employs a Q-Former [19] mechanism to compress visual features into a fixed number of tokens, which are then concatenated with text tokens. This approach facilitates the comprehension of visual and linguistic information through instruction tuning. (4) **LLaVA** [23] and (5) **MiniGPT-4** [48] use a linear projection layer for cross-modal embedding alignment. LLaVA emphasizes fine-tuning for visual-language alignment by specific instructions, while MiniGPT-4 is optimized for generating detailed descriptions from images. (6) **LLaVA-v1.5** [22] and (7) **MiniGPT-v2** [7] are the improved version of the original model, optimized for better cross-modal understanding. (8) **Osprey** [43] introduces a mask-based visual extractor to extract features from high-resolution images, enabling fine-grained and open-world visual understanding. (9)

Table 3: Performance of LVLMs and hallucination mitigation methods on the POPE dataset. The best results are highlighted in bold. The subscript values indicate the improvement over the backbone models.

Model	Accuracy	Precision	Recall	F1
mPLUG-Owl	50.67	50.34	99.33	66.82
Multi-modal-GPT	50.00	50.00	100.00	66.67
InstructBLIP	74.37	67.67	93.33	78.45
LLaVA	50.77	50.39	99.87	66.98
Osprey	85.33	85.43	85.20	85.31
GLaMM	87.30	85.03	90.53	87.70
LLaVA-v1.5	85.17	89.93	79.20	84.23
+ HA-DPO	81.46 _[-3.71]	77.99 _[-11.94]	87.66 _[+8.46]	82.54 _[-1.69]
+ HA-CL	86.54 _[+1.37]	93.01 _[+3.08]	79.52 _[+0.32]	85.73 _[+1.50]
+ Hard Prompt	89.93 _[+4.76]	91.14 _[+1.21]	88.47 _[+9.27]	89.78 _[+5.55]
+ PATCH (ours)	90.20 _[+5.03]	91.13 _[+1.20]	89.07 _[+9.87]	90.09 _[+5.86]
MiniGPT-4	57.67	54.29	96.93	69.60
+ HA-DPO	75.66 _[+17.99]	74.36 _[+20.07]	78.33 _[-18.60]	76.29 _[+6.69]
+ Woodpecker	82.33 _[+24.66]	83.92 _[+29.63]	80.00 _[-16.93]	81.91 _[+12.31]
+ HA-CL	71.32 _[+13.65]	70.53 _[+16.24]	73.45 _[-23.48]	71.96 _[+2.36]
+ Hard Prompt	70.73 _[+13.06]	63.60 _[+9.31]	96.93 _[+0.00]	76.81 _[+7.21]
+ PATCH (ours)	88.13 _[+30.46]	86.99 _[+32.70]	89.67 _[-7.26]	88.31 _[+18.71]
MiniGPT-v2	83.33	88.28	76.87	82.18
+ Hard Prompt	88.77 _[+5.44]	88.23 _[-0.05]	89.47 _[+12.60]	88.84 _[+6.66]
+ PATCH (ours)	90.03 _[+6.70]	91.39 _[+3.11]	88.40 _[+11.53]	89.87 _[+7.69]

GLaMM [29] is the first model capable of generating natural language responses intertwined with corresponding object segmentation masks, enabling in-depth region understanding.

In addition to these LVLMs, we compare our method with three recently released hallucination-solving methods based on LLaVA-v1.5 and MiniGPT-4: (1) **HA-DPO** [46] reformulates the hallucination problem as a preference optimization task, training the model to consistently favor the accurate responses over hallucinatory ones with the given image-question pair. (2) **Woodpecker** [41] proposes a five-stage framework to locate the hallucinations and verify factuality, introducing a training-free method to correct hallucinations from the generated texts. (3) **HA-CL** [17] incorporates contrastive learning into the training process by treating hallucinatory text as hard negative examples, encouraging the model to align non-hallucinatory texts more closely with their corresponding images.

5.4 Experimental Results

Analysis on POPE. The experimental results are shown in Table 3. It is clear to see that our method significantly improves the performance of three backbone LVLMs in the object hallucination recognition task. Several observations emerge from the results: (1) Pre-trained LVLMs, such as mPLUG-Owl, Multi-modal-GPT, InstructBLIP, MiniGPT-4, and LLaVA are prone to generate hallucinated content, while their advanced versions (LLaVA-v1.5 and MiniGPT-v2) exhibit better performance. We attribute this to their superior training strategies (*i.e.*, instruction tuning). Models with pixel-level understanding, such as Osprey and GLaMM, perform relatively well on POPE, likely benefiting from the incorporation of extensive object-level instruction data during training. (2) Both Hard Prompt and PATCH improve the backbone performance, confirming that incorporating object-related information aids LVLMs in better interpreting visual features. Specifically, PATCH outperforms

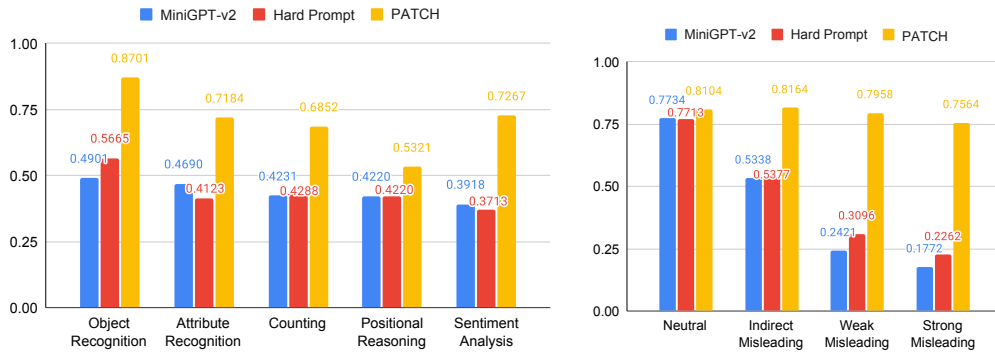


Figure 2: Performance on the PhD dataset across different task types (left) and conflict levels (right).

Table 4: The ablation results on object-related information and virtual token position on the POPE dataset, where “categ.” denotes categories.

Method	Accuracy	Precision	Recall	F1
PATCH	90.03	91.39	88.40	89.87
w/o bbox	88.27	87.37	89.47	88.41
w/o bbox & categ.	82.60	84.93	79.27	82.00
w/ Late	87.60	85.79	90.13	87.91

Hard Prompt as the parameters of virtual tokens are optimized during fine-tuning, allowing precise alignment between image content and corresponding texts, which effectively mitigates object hallucinations in LLMs. (3) Compared to three previous approaches designed to alleviate object hallucinations, PATCH achieves notable accuracy improvements of 30.46%, 5.03%, and 6.70% on LLaVA-v1.5, MiniGPT-4 and MiniGPT-v2, respectively, achieving the state-of-the-art performance. Unlike HA-DPO and HACL, which rely on complex optimization techniques, PATCH achieves superior results with minimal parameter tuning. While Woodpecker proposes a training-free solution, its reliance on manually crafted prompts limits its flexibility and scalability. In contrast, PATCH introduces a parameter-efficient fine-tuning strategy via pluggable virtual tokens, enabling the model to adaptively extract valuable information from detection information during the fine-tuning process.

Analysis on PhD. We compare PATCH with the Hard Prompt method based on MiniGPT-v2 across different task types and conflict levels on the PhD dataset: (1) **Task types.** The accuracy scores of the three variants across five task types are presented on the left side of Figure 2. The results show that using the Hard prompt to inject object-related information can improve performance in object recognition, counting, and positional reasoning tasks. This is consistent with our findings in preliminary experiments, where object-related information enhances the LLM’s understanding of geometric information of objects in images. However, for object attribute recognition and sentiment analysis tasks, the hard prompt brings some negative effects. This may be due to the fact that the detection results do not include information directly relevant to the given questions. Consequently, inserting complex object-related

Table 5: Experimental results by replacing the object categories with the generic placeholder.

Method	Accuracy	Precision	Recall	F1
MiniGPT-v2	83.37	88.00	77.27	82.29
w/ placeholder	80.70	86.40	72.87	79.06
PATCH	90.03	91.39	88.40	89.87
w/ placeholder	88.73	88.89	88.53	88.71

information into the input texts may introduce excessive redundant noise, interfering with the ability of LLMs to effectively leverage their prior knowledge. Fortunately, PATCH improves performance across all tasks, which clearly demonstrates that the fine-tuned virtual tokens can effectively guide the model in extracting valuable information from detection results as well as mining the prior knowledge within the LLM. (2) **Conflict levels.** On the right side of Figure 2, we present the accuracy scores of the three variants across four conflict levels. The PhD dataset provides three statements per question that are entirely inconsistent with the image content, serving as misleading context to challenge the model during answer generation. The misleading statements are categorized into three types based on their intensity: strong misleading, weak misleading, and indirect misleading, while neutral represents the original question text without added misleading statement. From the results, it is obvious that the three variants perform similarly on neutral questions, indicating that recent pre-trained LLMs are able to answer questions accurately in the absence of misleading information. However, as misleading statements are introduced into the context, the performance of MiniGPT-v2 and Hard Prompt declines significantly. This suggests that LLMs struggle to handle questions with misleading texts, and simply adding object-related information as prompts is insufficient to mitigate this issue. In contrast, the proposed PATCH performs remarkably well even on strongly misleading questions, showing that fine-tuning LLMs with trainable virtual tokens can effectively improve the model’s ability to discern the true relationships between textual and visual content. This demonstrates the robust cross-modal information understanding capability of PATCH, showcasing its effectiveness in addressing the object hallucination issue in LLMs.

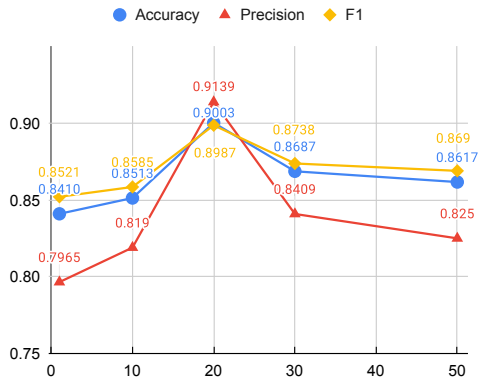


Figure 3: Accuracy, Precision, and F1 score over different token quantities on POPE dataset.

5.5 Ablation Study

5.5.1 Impact on Object-related Information. (1) **Recognition Information.** We explore the impact of various object detection results on PATCH, and the experimental results are shown in Table 4. The “bboxes” is denoted as the bounding box information and “categ.” represents the object category information. The experimental results show that when complete detection information is provided, PATCH achieves the highest accuracy of 90.03% on the POPE dataset, demonstrating its effectiveness in enhancing LVLMs’ understanding of scenes and objects. When the bounding box information is removed, the accuracy drops by 1.76%, suggesting that bounding boxes play an important role in object localization and scene comprehension. However, a slight increase in the recall score is observed at the same time, suggesting that without bounding boxes, the model becomes more effective at detecting positive samples. This may be because bounding boxes sometimes cause the model to focus narrowly on specific regions, thereby limiting its understanding of the broader image context. When all object-related information is omitted, leaving only 20 trainable virtual tokens for fine-tuning, the model’s performance drops significantly. This indicates that without the additional object-related information, solely fine-tuning virtual tokens is insufficient to achieve consistent semantic alignment between visual and textual features. Consequently, the model exhibits increased uncertainty in object recognition, underscoring the importance of incorporating rich object-related information to mitigate hallucination in LVLMs. (2) **Impact of Token Position.** In our method, virtual tokens are added between the detection results and the question, following the format: “[Image][VirtualTokens][Object][Question]”. To investigate the effect of virtual token positioning, we consider an alternative format: “[Image][Object][VirtualTokens][Question]”, referred to as “PATCH w/ Late”. The comparison result is shown in Table 4, which indicates that the placement of the virtual tokens significantly impacts model performance. Positioning the virtual tokens between the object-related information and the image features enables the LVM to better interpret the detection information. In contrast, placing the virtual tokens after the object-related information causes the LVM to focus excessively on the detection

Table 6: Ablation experimental results over different token quantities on POPE dataset based on MiniGPT-v2.

	Accuracy	Precision	Recall	F1
MiniGPT-v2	83.37	88.00	77.27	82.29
+ 20 tokens	82.60	84.93	79.27	82.00
+ 30 tokens	82.27	82.97	81.20	82.08
+ 50 tokens	81.40	78.72	86.07	82.23
+ 100 tokens	77.67	73.29	87.07	79.59

Table 7: Ablation experimental results on different virtual token initializations on POPE dataset.

Initialization	Accuracy	Precision	Recall	F1
Random	86.77	84.28	90.40	87.23
T_1	88.83	93.76	83.20	88.17
T_2	90.03	91.39	88.40	89.87

text, while neglecting critical contextual cues from the overall image features, resulting in a performance decline. (3) **Impact of Localization Information.** Table 5 exhibits the ablation experimental results by replacing the object categories with a generic placeholder “object{idx}” to validate the effect of the localization information, where the object-related information is reformatted as object{idx}{<x1><x2><x3><x4>}. The experimental results demonstrate that merely incorporating object location information into LVLMs for reasoning fails to effectively mitigate hallucinations, likely due to the ambiguous referential details in the additional textual inputs. In contrast, when only location information is utilized for PATCH fine-tuning, hallucinations are partially mitigated. This may be attributed to the fact that the LVM learns to leverage virtual tokens to comprehend precise object localization information during the fine-tuning process, thereby enhancing image interpretation and ensuring faithful responses to the input image.

5.5.2 Impact on Token Quantities. We first evaluate the performance of PATCH across different quantities of virtual tokens. As illustrated in Figure 3, the metric scores initially improve as the number of virtual tokens increases, reaching optimal accuracy with 20 tokens, which yields a 6.70% improvement over the baseline configuration. However, further increasing the number of tokens results in a noticeable performance decline. This suggests that an excessive number of tokens may introduce redundant information, diminishing the model’s ability to accurately focus on essential object-related information, and ultimately leading to a significant degradation in overall performance. Then, we further explore the impact of virtual token quantities when object-related information is explicitly excluded based on MiniGPT-v2. The experimental results are shown in Table 6, which clearly demonstrate the critical role of the incorporation of the detection results. These findings suggest that simply increasing the number of trainable prompting tokens is insufficient to mitigate hallucinations in LVLMs. Moreover, an increased number of virtual tokens raises the fine-tuning costs, leading to a gradual decline in performance when the learning rate and number of training epochs remain fixed.

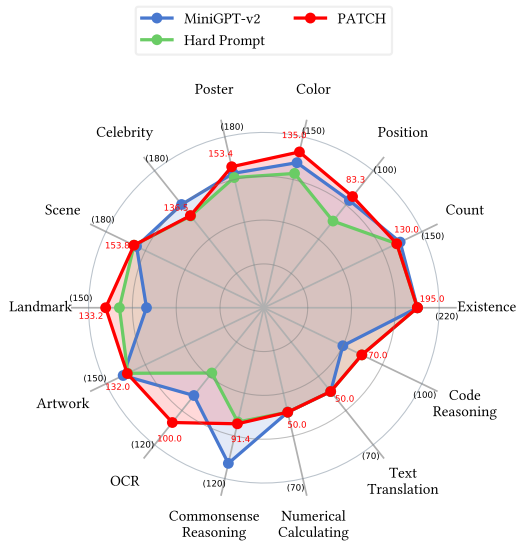


Figure 4: Performance of MiniGPT-v2, Hard Prompt and PATCH on MME benchmark across 14 subtasks.

5.5.3 Impact on the Initialization Strategy of Virtual Tokens. To investigate the effect on the initialization format of virtual tokens, we introduced two distinct strategies: (1) **Random Initialization** and (2) **Text-based Initialization** which consists of two instruction texts. The template of T_1 refers to “According to the previous object detection results, please answer the following question”, while T_2 refers to “According to the previous object detection results, please answer the following question with ‘yes’ or ‘no’”. The text encoder of the LVLM is leveraged to encode the input prompt, which is configured with a maximum sequence length of n . Sequences exceeding this limit are truncated, while shorter sequences are zero-padded to ensure dimensional consistency across all inputs. The experimental results of PATCH are shown in Table 7, which indicates that random initialization leads to a noticeable decrease in overall model performance. In contrast, initializing tokens with explicit text-based prompts consistently improves all evaluation metrics. Given that the responses in the POPE dataset are constrained to “yes” or “no”, aligning virtual token initialization with the answer distribution enhances the LVLM’s ability to effectively utilize virtual tokens for extracting relevant object-related information, resulting in more reliable and standardized response generation.

5.6 Further Analysis

Performance on MME Evaluation Benchmark. We conduct an experiment on the multi-modal evaluation benchmark, MME [13], to assess PATCH’s effectiveness in general-domain tasks. Specifically, PATCH is initialized with parameters pre-trained on the POPE (AOKVQA-version) dataset. Table 8 and Figure 4 summarize the performance across the Perception and Cognition tasks in MME. Experimental results demonstrate that PATCH outperforms MiniGPT-v2 by 34.55 points in the Perception task, with particularly strong performance in Position, Color, Poster, Scene, Landmark, and OCR tasks. This improvement is primarily attributed to PATCH’s

Table 8: Overall performance on MME benchmark in Perception and Cognition tasks.

Method	Perception	Cognition
MiniGPT-v2	1317.45	269.64
+ Hard Prompt	1290.96	260.71
+ PATCH	1352.2	261.43

Table 9: Zero-shot experimental results of PATCH on the full PhD dataset using parameters pre-trained on POPE dataset.

Method	Accuracy	Precision	Recall	F1
MiniGPT-v2	47.92	52.46	55.48	53.93
+ Hard Prompt	49.48	53.20	66.86	59.25
+ PATCH	52.84	55.91	66.90	60.91

enhanced alignment with image contents. However, performance declines in Count, Celebrity, and Artwork tasks, which is likely due to the detector errors and the model’s limited understanding of celebrity-related information. These limitations could potentially be mitigated through improved object detectors and retrieval-augmented generation techniques. Despite these improvements, PATCH exhibits an 8.21-point performance decrease on the Cognition task. Since our method has only been fine-tuned on the POPE (AOKVQA-version) dataset, we believe that additional fine-tuning on larger-scale datasets could further enhance its performance.

Zero-shot Experiment. PATCH, initialized with parameters fine-tuned on the POPE (AOKVQA-version) dataset, is evaluated on the full PhD dataset. To ensure the validity, we have thoroughly verified that there is no distribution overlap between the two datasets. The experimental results are shown in Table 9, which demonstrate a 4.92% improvement in accuracy over the baseline model. This observation further validates PATCH’s plug-and-play capability, as it can be directly transferred to a new dataset without additional fine-tuning while still delivering significant performance gains.

6 Conclusion

In this paper, we revisit hallucinations in LVLMs from an architectural perspective, hypothesizing two potential causes: (1) insufficient extraction of visual features and (2) inadequate decoupling of visual features. Based on our preliminary experimental results, we identify that the primary cause lies in insufficient cross-modal alignment rather than deficiencies in the visual encoding process. Motivated by this insight, we propose PATCH, a novel parameter-efficient fine-tuning strategy, which employs several learnable virtual tokens to effectively bridge the semantic gap between the image features, object-related information augmented prompts, and input questions. By incorporating the fine-tuned virtual tokens into the LVLM vocabulary, PATCH is able to be utilized as a versatile plug-and-play method for diverse applications. Extensive experiments on three publicly available hallucination evaluation benchmarks demonstrate the effectiveness and generalization of our approach in resisting various levels of misleading contextual interference and mitigating the object hallucination issue in LVLMs.

References

- [1] Jean-Baptiste Alayrac, Jeff Donahue, Pauline Luc, Antoine Miech, Iain Barr, Yana Hasson, Karel Lenc, Arthur Mensch, Katherine Millican, Malcolm Reynolds, et al. 2022. Flamingo: a visual language model for few-shot learning. *Advances in neural information processing systems* 35 (2022), 23716–23736.
- [2] Zechen Bai, Pichao Wang, Tianjun Xiao, Tong He, Zongbo Han, Zheng Zhang, and Mike Zheng Shou. 2024. Hallucination of multimodal large language models: A survey. *arXiv preprint arXiv:2404.18930* (2024).
- [3] Zhaowei Cai and Nuno Vasconcelos. 2021. Cascade R-CNN: High Quality Object Detection and Instance Segmentation. *IEEE Transactions on Pattern Analysis and Machine Intelligence* 43, 5 (2021), 1483–1498.
- [4] Boyuan Chen, Zhuo Xu, Sean Kirmani, Brain Ichter, Dorsa Sadigh, Leonidas Guibas, and Fei Xia. 2024. Spatialvlm: Endowing vision-language models with spatial reasoning capabilities. In *Proceedings of the IEEE/CVF Conference on Computer Vision and Pattern Recognition*. 14455–14465.
- [5] Jiawei Chen, Zhengwei Fang, Xiao Yang, Chao Yu, Zhaoxia Yin, and Hang Su. 2025. Exploring the Secondary Risks of Large Language Models. *arXiv preprint arXiv:2506.12382* (2025).
- [6] Jiawei Chen, Xiao Yang, Zhengwei Fang, Yu Tian, Yinpeng Dong, Zhaoxia Yin, and Hang Su. 2024. Autoreach: Universal and adaptive jailbreaking with efficient wordplay-guided optimization. *arXiv preprint arXiv:2405.19668* (2024).
- [7] Jun Chen, Deyao Zhu, Xiaoqian Shen, Xiang Li, Zechun Liu, Pengchuan Zhang, Raghuraman Krishnamoorthi, Vikas Chandra, Yunyang Xiong, and Mohamed Elhoseiny. 2023. Minigt-v2: large language model as a unified interface for vision-language multi-task learning. *arXiv preprint arXiv:2310.09478* (2023).
- [8] Lin Chen, Jisong Li, Xiaoyi Dong, Pan Zhang, Conghui He, Jiaqi Wang, Feng Zhao, and Dahua Lin. 2023. Sharegpt4v: Improving large multi-modal models with better captions. *arXiv preprint arXiv:2311.12793* (2023).
- [9] Wenliang Dai, Junnan Li, DONGXU LI, Anthony Tiong, Junqi Zhao, Weisheng Wang, Boyang Li, Pascale N Fung, and Steven Hoi. 2023. InstructBLIP: Towards General-purpose Vision-Language Models with Instruction Tuning. In *Advances in Neural Information Processing Systems*, Vol. 36. 49250–49267.
- [10] Jiajun Deng, Zhengyuan Yang, Tianlang Chen, Wengang Zhou, and Houqiang Li. 2021. TransVG: End-to-End Visual Grounding With Transformers. In *Proceedings of the IEEE/CVF International Conference on Computer Vision (ICCV)*. 1769–1779.
- [11] Alexey Dosovitskiy. 2020. An image is worth 16x16 words: Transformers for image recognition at scale. *arXiv preprint arXiv:2010.11929* (2020).
- [12] Yuxin Fang, Wen Wang, Binhui Xie, Quan Sun, Ledell Wu, Xinggang Wang, Tiejun Huang, Xinlong Wang, and Yue Cao. 2023. Eva: Exploring the limits of masked visual representation learning at scale. In *Proceedings of the IEEE/CVF Conference on Computer Vision and Pattern Recognition*. 19358–19369.
- [13] Chaoyou Fu, Peixian Chen, Yunhang Shen, Yulei Qin, Mengdan Zhang, Xu Lin, Jinrui Yang, Xiawu Zheng, Ke Li, Xing Sun, et al. 2023. MME: A Comprehensive Evaluation Benchmark for Multimodal Large Language Models. *arXiv preprint arXiv:2306.13394* (2023).
- [14] Tao Gong, Chengqi Lyu, Shilong Zhang, Yudong Wang, Miao Zheng, Qian Zhao, Kuikun Liu, Wenwei Zhang, Ping Luo, and Kai Chen. 2023. Multimodal-gpt: A vision and language model for dialogue with humans. *arXiv preprint arXiv:2305.04790* (2023).
- [15] Abdul Mueed Hafiz and Ghulam Mohiuddin Bhat. 2020. A survey on instance segmentation: state of the art. *International journal of multimedia information retrieval* 9, 3 (2020), 171–189.
- [16] Qidong Huang, Xiaoyi Dong, Pan Zhang, Bin Wang, Conghui He, Jiaqi Wang, Dahua Lin, Weiming Zhang, and Nenghai Yu. 2024. Opera: Alleviating hallucination in multi-modal large language models via over-trust penalty and retrospection-allocation. In *Proceedings of the IEEE/CVF Conference on Computer Vision and Pattern Recognition*. 13418–13427.
- [17] Chaoya Jiang, Haiyang Xu, Mengfan Dong, Jiaying Chen, Wei Ye, Ming Yan, Qinghao Ye, Ji Zhang, Fei Huang, and Shikun Zhang. 2024. Hallucination augmented contrastive learning for multimodal large language model. In *Proceedings of the IEEE/CVF Conference on Computer Vision and Pattern Recognition*. 27036–27046.
- [18] Liqiang Jing and Xinya Du. 2024. Fgaif: Aligning large vision-language models with fine-grained ai feedback. *arXiv preprint arXiv:2404.05046* (2024).
- [19] Junnan Li, Dongxu Li, Silvio Savarese, and Steven Hoi. 2023. Blip-2: Bootstrapping language-image pre-training with frozen image encoders and large language models. In *International conference on machine learning*. PMLR, 19730–19742.
- [20] Li Li, Jiawei Peng, Huiyi Chen, Chongyang Gao, and Xu Yang. 2024. How to Configure Good In-Context Sequence for Visual Question Answering. In *Proceedings of the IEEE/CVF Conference on Computer Vision and Pattern Recognition (CVPR)*. 26710–26720.
- [21] Yifan Li, Yifan Du, Kun Zhou, Jinpeng Wang, Wayne Xin Zhao, and Ji-Rong Wen. 2023. Evaluating Object Hallucination in Large Vision-Language Models. In *Proceedings of the 2023 Conference on Empirical Methods in Natural Language Processing*. 292–305.
- [22] Haotian Liu, Chunyuan Li, Yuheng Li, and Yong Jae Lee. 2024. Improved baselines with visual instruction tuning. In *Proceedings of the IEEE/CVF Conference on Computer Vision and Pattern Recognition*. 26296–26306.
- [23] Haotian Liu, Chunyuan Li, Qingyang Wu, and Yong Jae Lee. 2024. Visual instruction tuning. *Advances in neural information processing systems* 36 (2024).
- [24] Hanchao Liu, Wenyuan Xue, Yifei Chen, Dapeng Chen, Xiutian Zhao, Ke Wang, Liping Hou, Rongjun Li, and Wei Peng. 2024. A survey on hallucination in large vision-language models. *arXiv preprint arXiv:2402.00253* (2024).
- [25] Jiazhen Liu, Yuhan Fu, Ruobing Xie, Runqian Xie, Xingwu Sun, Fengzong Lian, Zhanhui Kang, and Xirong Li. 2024. Phd: A prompted visual hallucination evaluation dataset. *arXiv preprint arXiv:2403.11116* (2024).
- [26] Shuyuan Liu, Jiawei Chen, Shouwei Ruan, Hang Su, and Zhaoxia Yin. 2024. Exploring the robustness of decision-level through adversarial attacks on llm-based embodied models. In *Proceedings of the 32nd ACM International Conference on Multimedia*. 8120–8128.
- [27] Ilya Loshchilov and Frank Hutter. 2016. Sgdr: Stochastic gradient descent with warm restarts. *arXiv preprint arXiv:1608.03983* (2016).
- [28] Alec Radford, Jong Wook Kim, Chris Hallacy, Aditya Ramesh, Gabriel Goh, Sandhini Agarwal, Girish Sastry, Amanda Askell, Pamela Mishkin, Jack Clark, et al. 2021. Learning transferable visual models from natural language supervision. In *International conference on machine learning*. PMLR, 8748–8763.
- [29] Hanoona Rasheed, Muhammad Maaz, Sahal Shaji, Abdelrahman Shaker, Salman Khan, Hisham Cholakkal, Rao M Anwer, Eric Xing, Ming-Hsuan Yang, and Fahad S Khan. 2024. Glamm: Pixel grounding large multimodal model. In *Proceedings of the IEEE/CVF Conference on Computer Vision and Pattern Recognition*. 13009–13018.
- [30] Matteo Stefanini, Marcella Cornia, Lorenzo Baraldi, Silvia Cascianelli, Giuseppe Fiameni, and Rita Cucchiara. 2022. From show to tell: A survey on deep learning-based image captioning. *IEEE transactions on pattern analysis and machine intelligence* 45, 1 (2022), 539–559.
- [31] Quan Sun, Yuxin Fang, Ledell Wu, Xinlong Wang, and Yue Cao. 2023. Eva-clip: Improved training techniques for clip at scale. *arXiv preprint arXiv:2303.15389* (2023).
- [32] Zhiqing Sun, Sheng Shen, Shengcao Cao, Haotian Liu, Chunyuan Li, Yikang Shen, Chuang Gan, Liang-Yan Gui, Yu-Xiong Wang, Yiming Yang, et al. 2023. Aligning large multimodal models with factually augmented rlhf. *arXiv preprint arXiv:2309.14525* (2023).
- [33] Ilya O Tolstikhin, Neil Houlsby, Alexander Kolesnikov, Lucas Beyer, Xiaohua Zhai, Thomas Unterthiner, Jessica Yung, Andreas Steiner, Daniel Keysers, Jakob Uszkoreit, et al. 2021. Mlp-mixer: An all-mlp architecture for vision. *Advances in neural information processing systems* 34 (2021), 24261–24272.
- [34] Shengbang Tong, Zhuang Liu, Yuexiang Zhai, Yi Ma, Yann LeCun, and Saining Xie. 2024. Eyes wide shut? exploring the visual shortcomings of multimodal llms. In *Proceedings of the IEEE/CVF Conference on Computer Vision and Pattern Recognition*. 9568–9578.
- [35] Hugo Touvron, Thibaut Lavril, Gautier Izacard, Xavier Martinet, Marie-Anne Lachaux, Timothée Lacroix, Baptiste Rozière, Naman Goyal, Eric Hambro, Faisal Azhar, et al. 2023. Llama: Open and efficient foundation language models. *arXiv preprint arXiv:2302.13971* (2023).
- [36] Hugo Touvron, Louis Martin, Kevin Stone, Peter Albert, Amjad Almahairi, Yasmin Babaei, Nikolay Bashlykov, Soumya Batra, Prajwal Bhargava, Shrubti Bhosale, et al. 2023. Llama 2: Open foundation and fine-tuned chat models. *arXiv preprint arXiv:2307.09288* (2023).
- [37] Peng Xu, Wenqi Shao, Kaipeng Zhang, Peng Gao, Shuo Liu, Meng Lei, Fanqing Meng, Siyuan Huang, Yu Qiao, and Ping Luo. 2023. Lvlm-ehub: A comprehensive evaluation benchmark for large vision-language models. *arXiv preprint arXiv:2306.09265* (2023).
- [38] Peng Xu, Wenqi Shao, Kaipeng Zhang, Peng Gao, Shuo Liu, Meng Lei, Fanqing Meng, Siyuan Huang, Yu Qiao, and Ping Luo. 2024. Lvlm-ehub: A comprehensive evaluation benchmark for large vision-language models. *IEEE Transactions on Pattern Analysis and Machine Intelligence* (2024).
- [39] Dingchen Yang, Bowen Cao, Guang Chen, and Changjun Jiang. 2024. Pen-sieve: Retrospect-then-compare mitigates visual hallucination. *arXiv preprint arXiv:2403.14401* (2024).
- [40] Qinghao Ye, Haiyang Xu, Guohai Xu, Jiabo Ye, Ming Yan, Yiyang Zhou, Junyang Wang, Anwen Hu, Pengcheng Shi, Yaya Shi, et al. 2023. mplug-owl: Modularization empowers large language models with multimodality. *arXiv preprint arXiv:2304.14178* (2023).
- [41] Shukang Yin, Chaoyou Fu, Sirui Zhao, Tong Xu, Hao Wang, Dianbo Sui, Yunhang Shen, Ke Li, Xing Sun, and Enhong Chen. 2023. Woodpecker: Hallucination correction for multimodal large language models. *arXiv preprint arXiv:2310.16045* (2023).
- [42] Qifan Yu, Juncheng Li, Longhui Wei, Liang Pang, Wentao Ye, Bosheng Qin, Siliang Tang, Qi Tian, and Yueting Zhuang. 2024. HalluciDoctor: Mitigating Hallucinatory Toxicity in Visual Instruction Data. In *Proceedings of the IEEE/CVF Conference on Computer Vision and Pattern Recognition (CVPR)*. 12944–12953.
- [43] Yuqian Yuan, Wentong Li, Jian Liu, Dongqi Tang, Xinjie Luo, Chi Qin, Lei Zhang, and Jianke Zhu. 2024. Osprey: Pixel Understanding with Visual Instruction Tuning. In *IEEE/CVF Conference on Computer Vision and Pattern Recognition, CVPR 2024*. IEEE, 28202–28211.

- [44] Jingyi Zhang, Jiaxing Huang, Sheng Jin, and Shijian Lu. 2024. Vision-Language Models for Vision Tasks: A Survey. *IEEE Transactions on Pattern Analysis and Machine Intelligence* 46, 8 (2024), 5625–5644.
- [45] Yi-Fan Zhang, Weichen Yu, Qingsong Wen, Xue Wang, Zhang Zhang, Liang Wang, Rong Jin, and Tieniu Tan. 2024. Debiasing large visual language models. *arXiv preprint arXiv:2403.05262* (2024).
- [46] Zhiyuan Zhao, Bin Wang, Linke Ouyang, Xiaoyi Dong, Jiaqi Wang, and Conghui He. 2023. Beyond hallucinations: Enhancing vlms through hallucination-aware direct preference optimization. *arXiv preprint arXiv:2311.16839* (2023).
- [47] Yiyang Zhou, Chenhang Cui, Jaehong Yoon, Linjun Zhang, Zhun Deng, Chelsea Finn, Mohit Bansal, and Huaxiu Yao. 2023. Analyzing and mitigating object hallucination in large vision-language models. *arXiv preprint arXiv:2310.00754* (2023).
- [48] Deyao Zhu, Jun Chen, Xiaoqian Shen, Xiang Li, and Mohamed Elhoseiny. 2023. Minigt-4: Enhancing vision-language understanding with advanced large language models. *arXiv preprint arXiv:2304.10592* (2023).
- [49] Yutao Zhu, Zhaoheng Huang, Zhicheng Dou, and Ji-Rong Wen. 2024. One Token Can Help! Learning Scalable and Pluggable Virtual Tokens for Retrieval-Augmented Large Language Models. *arXiv preprint arXiv:2405.19670* (2024).

A Datasets

POPE [21]. The POPE dataset is specifically designed for object hallucination evaluation, introducing an adversarial setting for dataset construction. As illustrated in Figure 5, each sample consists of an image-question-answer pair. Given an input image, POPE first employs the automatic segmentation tool SEEM [?] to identify present objects in each image as ground truth. Questions related to these objects are classified as positive samples, receiving a “yes” response. Conversely, questions involving frequently co-occurring objects that are absent from the image are treated as negative samples, with a “no” response. This design establishes a binary classification testbed for assessing models’ susceptibility to object hallucination.

PhD [25]. The PhD dataset is a newly introduced benchmark for evaluating multi-modal hallucinations in LVLMS, categorizing hallucinations into three types: Object and Attribute Hallucinations, Multi-modal Conflicting Hallucinations, and Counter-Common-Sense Hallucinations. Our experiments are conducted on 35,033 samples of the first two hallucination types. The Object and Attribute Hallucinations are divided into five subcategories: “Object Recognition”, “Attribute Recognition”, “Counting”, “Positional Reasoning”, and “Sentiment Analysis”. The Multi-modal Conflicting Hallucination questions are specifically crafted to deceive the model by misleading contexts, which classify conflict levels into four distinct categories: “Neutral”, “Indirect Misleading”, “Weak Misleading”, and “Strong Misleading”. Figure 6 and 7 illustrate the examples of corresponding question-answer pairs in the PhD dataset.

B Implementation Details

MiniGPT-4. [48] For the POPE dataset, we initialize the learning rate at $1e-4$ and the weight decay is set to 0.05 until the learning rate decays to $1e-5$. Training is conducted over 30 epochs with a batch size of 1 within 2 hours.

MiniGPT-v2. [7] We initialize the model’s parameter by the LoRA-fine-tuned [?] checkpoint. For the POPE dataset, the initial learning rate is set to $2e-3$, with a batch size of 1, and training is conducted over 30 epochs within 2 hours. For the PhD dataset, the initial learning rate is set to $1e-3$, with a batch size of 1, and training lasts for 35 epochs within 2.5 hours. The weight decay is set to 0.05 until the learning rate decays to $5e-6$.

LLaVA-v1.5. [22] For the POPE dataset, the initial learning rate is set to $8e-4$. Training is conducted with a batch size of 16 over 1 epoch, completed in less than 20 minutes.

C Attention Map for the Final Token in the Input Sequence

Figure 8 illustrates the visualization of the attention scores for the final token in the input sequence concerning the subsequent token across each layer of the LLM. The heatmap illustrates that when the queried object is included in the detection information, specific object embeddings exhibit higher scores, which indicates that our method is able to effectively enhance the semantic alignment through the use of virtual tokens.

D Analysis of the Detection Head

Building upon the findings presented in the preliminary experiment, we conduct an additional experiment by replacing the Prompt₁ with

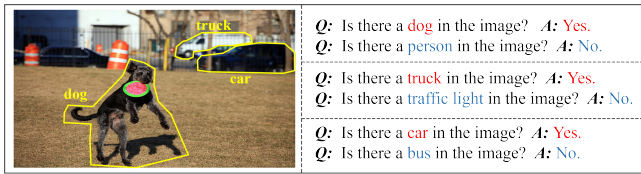


Figure 5: The example of question-answer pairs sampled under adversarial setting in the POPE dataset. Six questions are proposed for each image, three of which serve as positive samples. The corresponding negative samples are produced by replacing the object in each positive sample with a frequently co-occurring but absent object.



Figure 6: The examples of corresponding question-answer pairs across five task types in the PhD dataset.

Table 10: Comparison between the number of samples in detection and inference results conditioned on Prompt₂.

	Correct Inf.	Wrong Inf.
Correct Det.	2,670	97
Wrong Det.	56	240

Prompt₂, and the results are shown in Table 10. The comparison inference results on MiniGPT-v2 with the detection results reveals that incorporating object information into the LVLm effectively mitigates multi-modal hallucinations. Furthermore, the tabular results demonstrate consistent behavior between inference errors and detection errors after adding object-related information. We attribute these errors to the limitations of the detector’s performance, suggesting that using a more advanced detector could further enhance the performance of our method.



Figure 7: The examples of corresponding question-answer pairs across conflict levels in the PhD dataset.

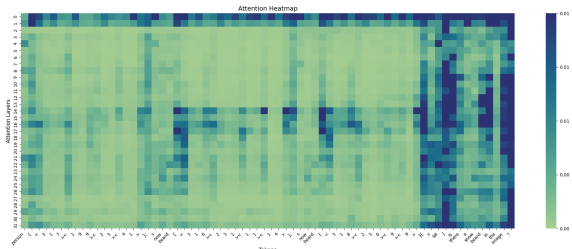


Figure 8: The visualization of attention scores across LLM layers based on PATCH.

E Limitations

Despite the success of PATCH in reducing hallucinations, our approach still faces the following limitations: (1) PATCH relies on the precision of the object-related detection results. Currently, due to the remarkable detection performance and transferability of Cascade Mask R-CNN [3], we adopt it as the visual detection head based on the configuration from EVA [12]. With the continuous development of object detection models, we believe that there will be potential to further enhance the robustness and effectiveness of our method. (2) When multiple instances of the same object appear in an image, the detection results may include duplicate object categories, which leads to an unnecessary increase in the LVLm input length. In the future, we plan to refine and optimize the detection prompting format to make it more simple and efficient for various complex real-world scenarios.